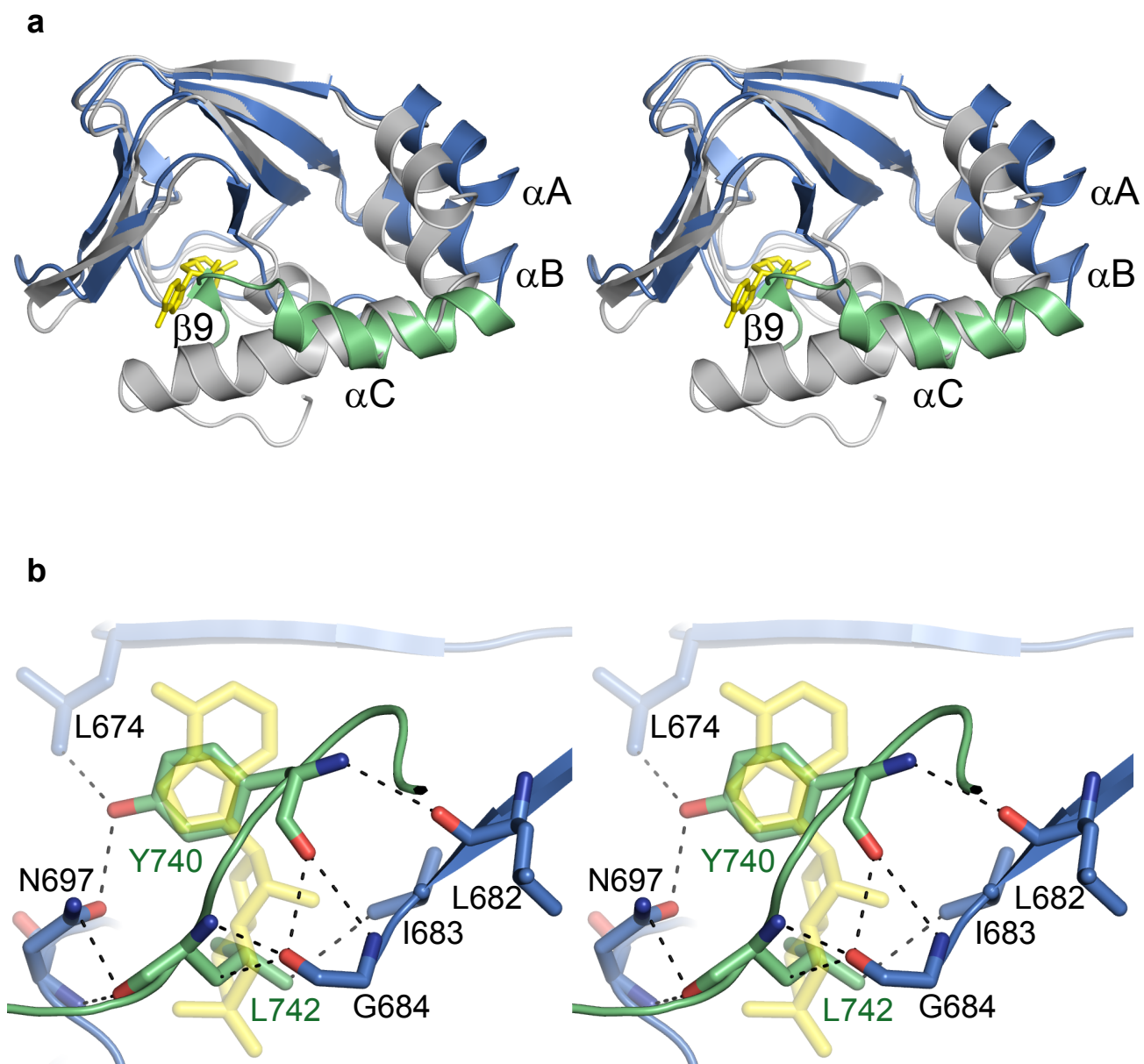
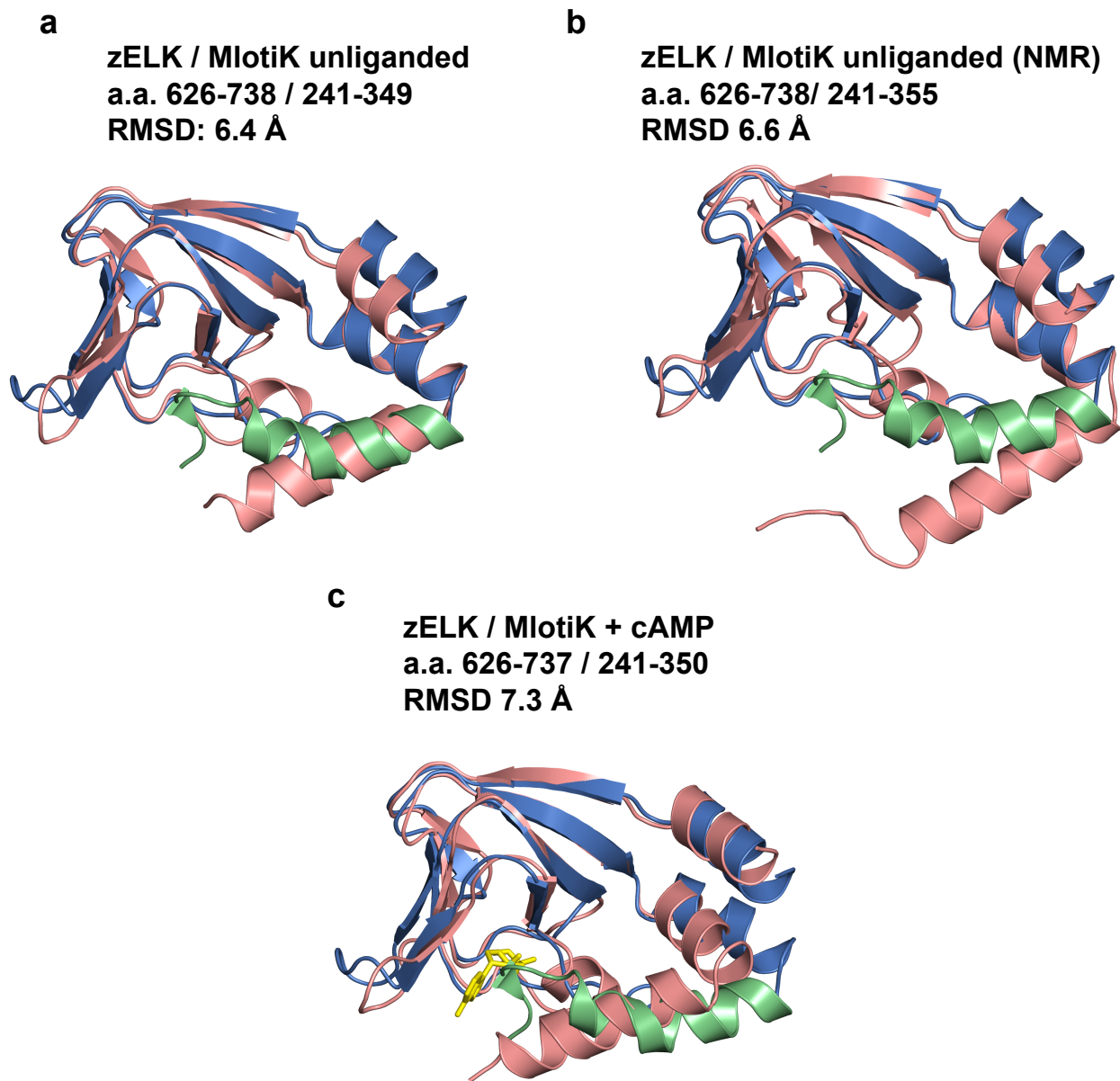


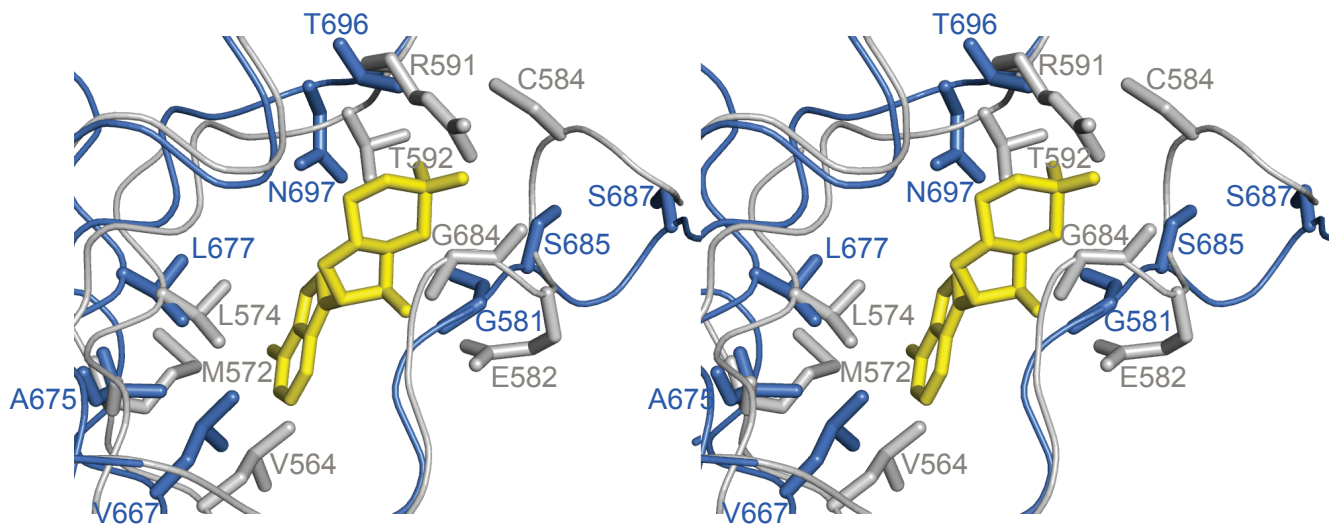
Supplementary Figure 1. Similarity of zELK channels to related ion channels. **a**, Phylogenetic tree, computed with Cobalt, showing the relationships of KCNH, CNG and HCN ion channel families. **b**, Conductance-voltage relations for zELK channels in the absence (black) and presence of 1 mM cAMP (red). Error bars indicate SEM (n=7). **c**, Amino acid sequence alignment of the C-terminal region of zELK and other ion channels in the KCNH, CNG and HCN ion channel families. The C-linker/CNBHD of zELK channels shares 83% amino acid sequence identity with hELK1 and 67% sequence identity with hELK2 channels. It also shares 42% identity with hERG and 36% identity with mEAG channels, but < 26% identity with HCN and CNG channels. Bars represent α -helices and arrows β -strands from the zELK structure.



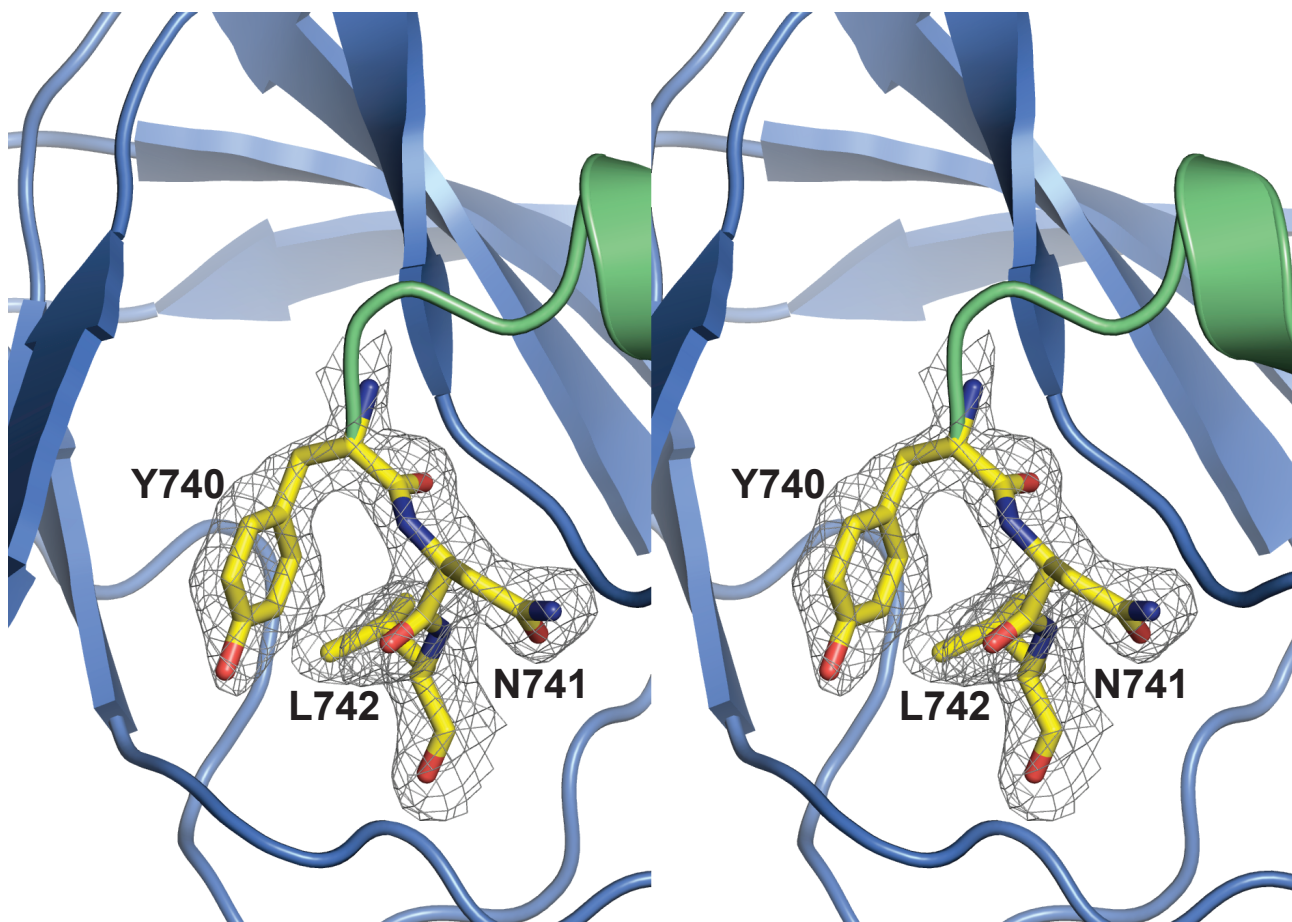
Supplementary Figure 2. Stereo view of the structurally aligned CNBHD of zELK and HCN2 channels, and residues in the β -roll cavity directly interacting with the intrinsic ligand. **a**, Stereo view of the alignment of the ribbon representations of the CNBHD of zELK (the α C helix is green and the rest of the CNBHD is blue) and HCN2 (grey) channels¹⁰. cAMP in the HCN2 structure is yellow. **b**, Stereo view of the residues in the β -roll cavity directly interacting with residues Y740 and L742 of the intrinsic ligand. cAMP in the structurally aligned, but not shown, CNBD of HCN2 channels is shown in yellow. Dashed lines show both polar and non-polar interactions.



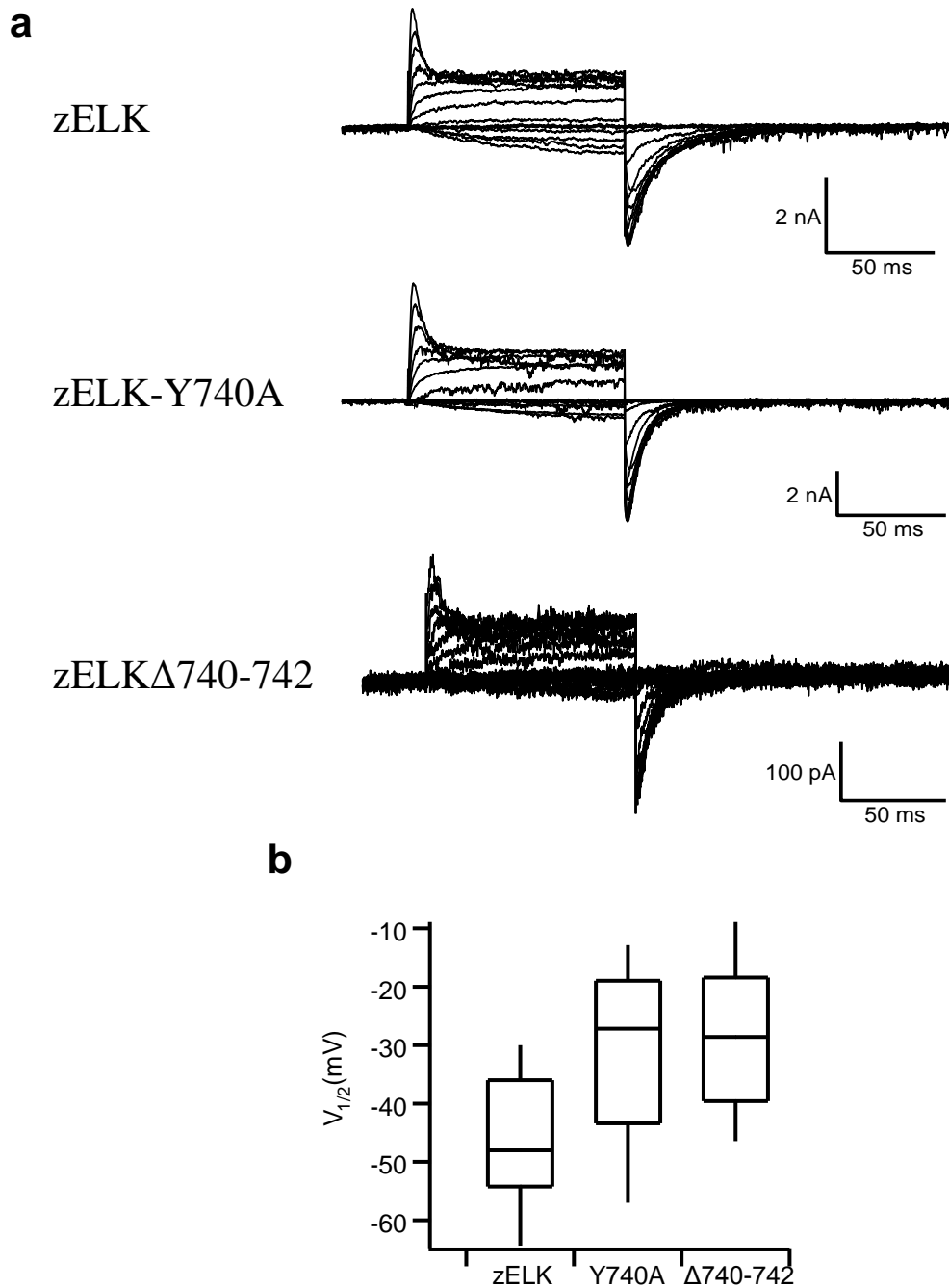
Supplementary Figure 3. Structural comparison of the CNBHD of zELK and CNBDs of MlotiK1 channels. a-c, Alignment of the ribbon representations of the CNBHD of zELK and unliganded crystal structure of the CNBD of MlotiK1 channels with R348A mutation²⁸ (a), unliganded NMR structure of the CNBD of MlotiK1²⁹ (b) and cAMP-bound crystal structure of the CNBD of MlotiK1 channels²⁸ (c). The α C helix of the CNBHD of zELK is green and the rest of the CNBHD is blue. The CNBD of MlotiK1 is pink. cAMP in the MlotiK1 structure is yellow. The corresponding PDB accession numbers for the MlotiK1 structures are 1U12 for (a), 2XKL for (b) and 1VP6 for (c). The RMSDs for the α carbons and the stretch of residues used for the RMSD calculations are indicated.



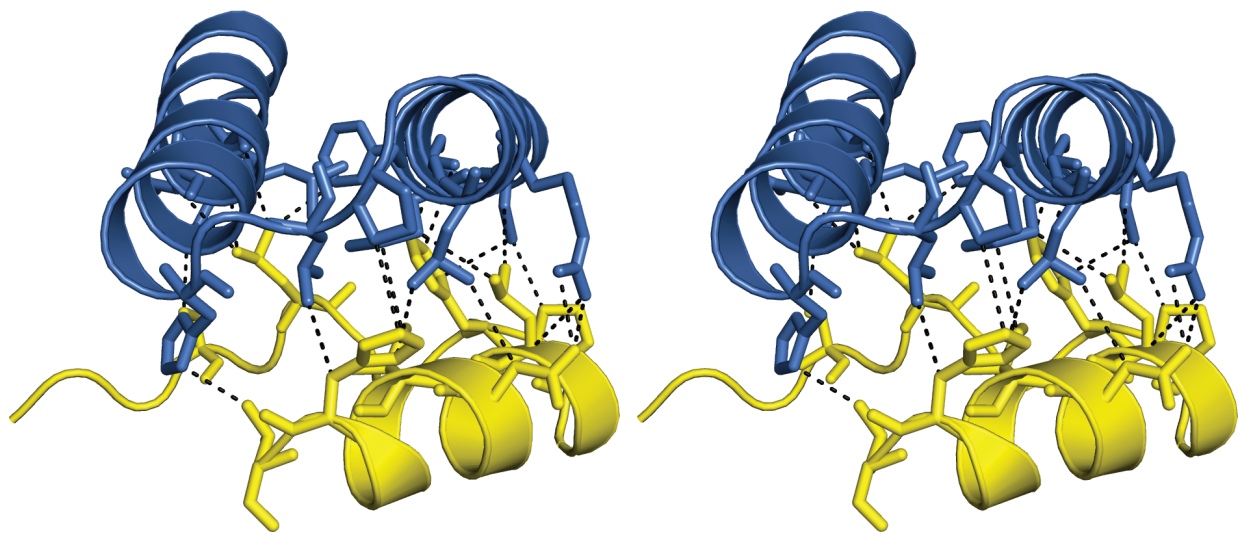
Supplementary Figure 4. Structural alignment of the β -roll cavity of the CNBHD of zELK (blue) and of the CNBD of HCN2 (grey) channels. Residues directly interacting with cAMP in the CNBD of HCN2 channels and their corresponding residues in the CNBHD of zELK channels are shown in sticks. Residues R632 and I636 in HCN2 channels were omitted from the figure because there are no corresponding residues in the same relative location in zELK channels.



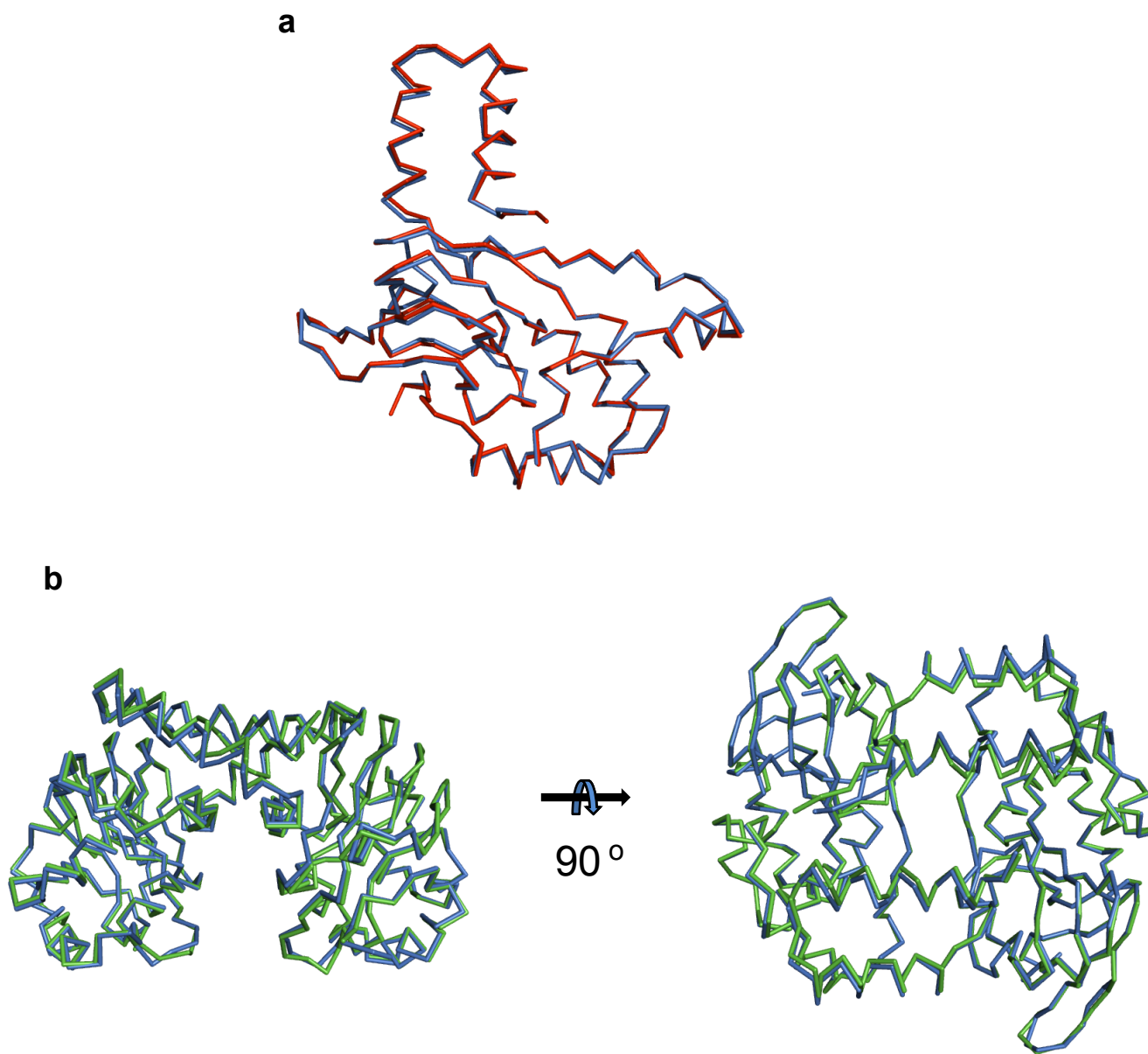
Supplementary Figure 5. Intrinsic ligand electron density. A 2Fo-Fc omit electron-density map of residues Y740-L742 of the intrinsic ligand bound inside the β -roll cavity of the CNBHD of zELK channels. The map is contoured at 1.0 σ .



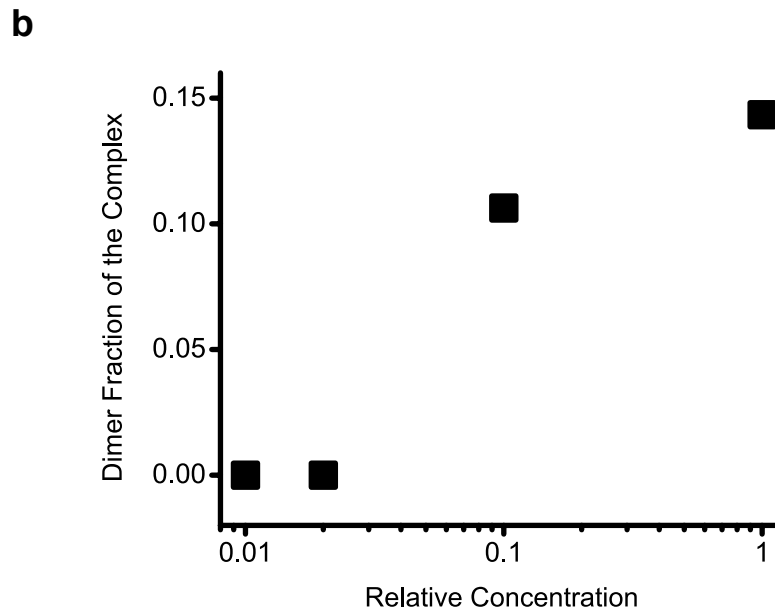
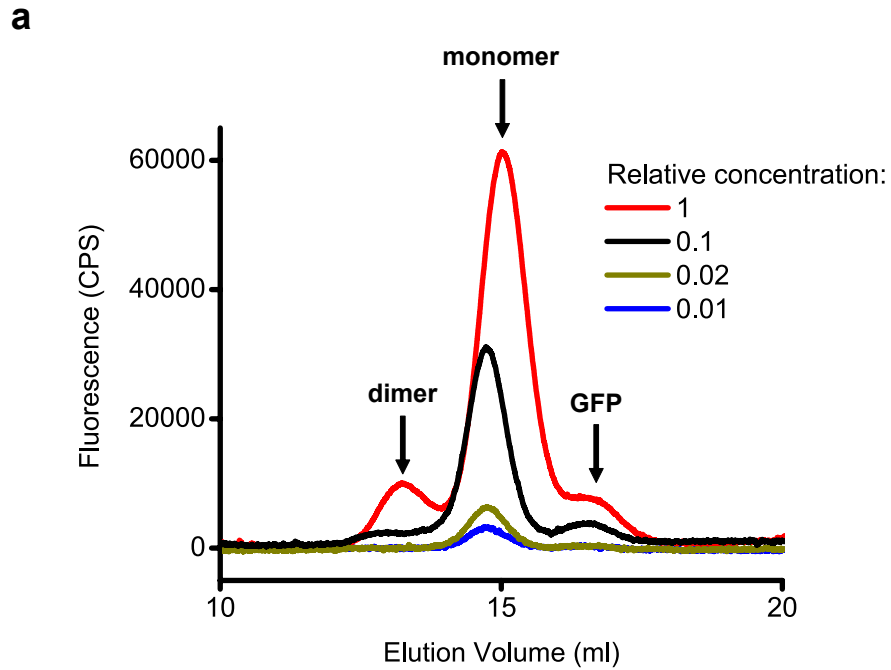
Supplementary Figure 6. Mutations of the β 9 strand shift the voltage dependence of activation to more depolarized voltages. **a**, Currents from wild-type, Y740A and Δ 740-742 mutant zELK channels. Currents were elicited by applying a series of 100 ms voltage pulses (ranging from -140 to +140 mV in 20 mV increments), followed by a 150 ms tail pulse to -100 mV. **b**, Box plot of $V_{1/2}$ values for wild-type, Y740A mutant, and Δ 740-742 mutant zELK channels. The line in the middle of the box represents the median, the box represents the 25th and 75th percentiles, and the “whiskers” represent the 5th and 95th percentiles of the data. For both mutations, the $V_{1/2}$ values for activation were significantly larger ($P < 0.01$, Student’s t -test) than the $V_{1/2}$ of wild-type channels (wild type: -45.3 ± 3.2 mV, $n = 18$; Y740A: -29.8 ± 4.4 mV, $n = 19$; Δ 740-742: -28.3 ± 4.4 mV, $n = 11$).



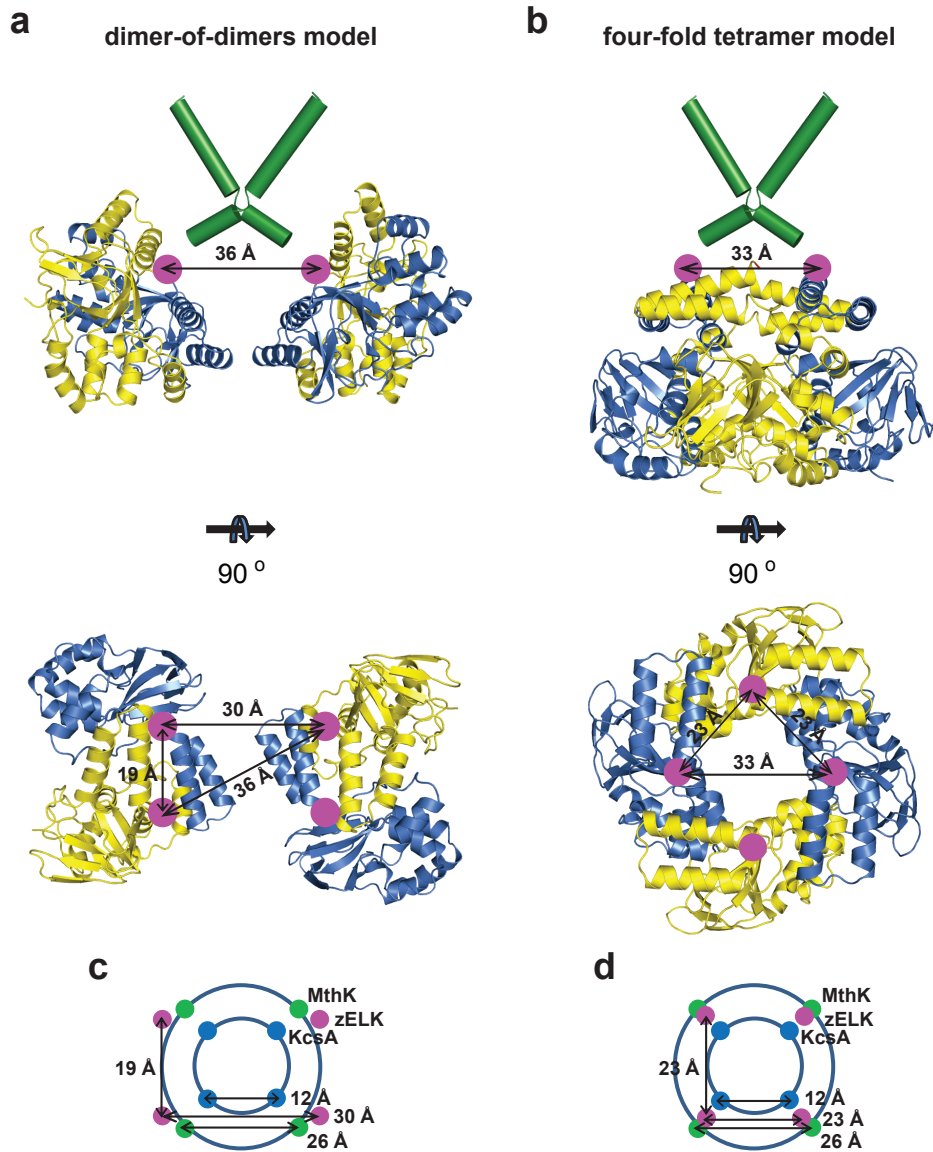
Supplementary Figure 7. Stereo view of the “elbow-on-the-shoulder” interface of zELK channels. The “elbow” is blue and the “shoulder” of the neighboring subunit is yellow. The residues forming the network of interactions between the “elbow” and the “shoulder” regions are shown in stick. Intersubunit contacts of less than 4 Å distance are shown as dashed lines for both polar and non-polar interactions.



Supplementary Figure 8. The structures and dimeric assembly are preserved for different monomers in the asymmetric unit and for both space groups of zELK crystals. a, Alignment of the backbone α -carbon traces of the C-linker/CNBHD monomers A (blue) and B (red) in $C222_1$ space group. b, Alignment of dimers formed by the C-linker/CNBHD of zELK channels in $C222_1$ (blue) and $P12_11$ (green) space groups viewed perpendicular (left) and parallel (right) to the two-fold axis.



Supplementary Figure 9. GFP-tagged C-linker/CNBHD of zELK channels dimerizes at sufficiently high concentrations in solution. **a**, FSEC profiles of the GFP-tagged C-linker/CNBHD of zELK channels for the indicated relative concentrations of the sample. The elution volumes of the dimer and monomer of the C-linker/CNBHD, as well as of the cleaved GFP, are indicated by the arrows. **b**, Plot of the fraction of the dimeric complex versus the relative concentration of the sample.



Supplementary Figure 10. Cartoons illustrating a possible dimer-of-dimers model and four-fold tetramer model for the arrangement of the C-linker/CNBHDs in the full-length zELK channel. a-b, A cartoon representation of two diagonally opposed inner-helices of the Kv1.2 (PDB 2A79)⁴⁴ channel docked to a dimer-of-dimers model (a) and a four-fold tetramer model (b) of the C-linker/CNBHDs of zELK channels viewed perpendicular (top) and parallel (bottom) to the Kv 1.2 pore axis. The Kv1.2 structure was omitted in the later for clarity. The dimer-of-dimers model was built by arranging two zELK dimers with a two-fold symmetry around the Kv1.2 pore axis. The four-fold tetramer model was built by modeling the C-linker from zELK after the C-linker from HCN2 (PDB 1Q5O)¹⁰ using SWISS-MODEL⁴⁰, and attaching the CNBHD of zELK. These monomers were then arranged with a four-fold symmetry around the Kv1.2 pore axis, as seen in HCN2 (PDB 1Q5O). The pink-colored spheres represent the amino-terminal residues of each of the zELK monomers in the models. The modeling was done in Pymol³⁷. (c,d) A schematic diagram comparing the proposed arrangements of the amino-termini of the C-linker/CNBHDs of zELK for a dimer-of-dimers model (c) and a four-fold tetramer model (d) with the corresponding arrangement for the carboxy-terminal residues of the inner helices of KcsA (PDB 1K4C)⁴² and MthK (PDB 1LNQ)⁴³ channels.

Supplementary Table 1: Data collection and refinement statistics

Crystal ID	T141 (SeMet)	T42 (Native)	T26 (Native)	T84 (Native)
Accession codes	3UK5	3UKN	3UKT	3UKV
Data collection				
Space group	C222 ₁	C222 ₁	P12 ₁ 1	P12 ₁ 1
Molecules / ACU	3	3	4	4
Cell dimensions				
<i>a</i> , <i>b</i> , <i>c</i> (Å)	58, 95.3, 241.4	58, 95.5, 241.2	55.7, 107.8, 77.58	55.33, 106.42, 77.52
α , β , γ (°)	90, 90, 90	90, 90, 90	90, 97.38, 90	90, 97.51, 90
Wavelength (Å)	0.979	1.000	1.000	1.000
Resolution (Å) ^a	45.80-2.50 (2.59-2.50)	49.56-2.20 (2.32-2.20)	76.94-2.30 (2.42-2.30)	48.76-2.70 (2.85-2.70)
<i>R</i> _{merge} (%)	8.1 (48.6)	6.2 (43.4)	4.1 (20.0)	6.6 (45.3)
<i>I</i> / σ <i>I</i>	13 (2.5)	9.9 (2.4)	12.5 (2.5)	8.1 (1.9)
Completeness (%)	97.4 (98)	97.6 (85.4)	93.1 (66.3)	99.8 (99.7)
Redundancy	3.7 (3.7)	4.4 (2.0)	3.2 (2.1)	3.5 (3.1)
Refinement				
Resolution (Å)	45.8 - 2.25	49.6 - 2.2	44.1 - 2.3	48.8 - 2.7
No. reflections	29786	33675	37513	23411
<i>R</i> _{work} / <i>R</i> _{free} (%) ^b	21.29 / 25.79	21.25 / 25.36	20.47 / 25.84	21.52 / 27.68
No. atoms				
Protein	4360	4396	5761	5261
Water	279	330	212	45
B-factors				
Protein	51.81	49.69	56.44	66.02
Water	46.42	45.73	51.64	55.56
R.m.s deviations				
Bond lengths (Å)	0.008	0.008	0.008	0.009
Bond angles (°)	1.149	1.092	1.072	1.253

^a Highest resolution shell is shown in parenthesis.^b 5% of data was set aside for calculation of *R*_{free}.

SUPPLEMENTARY DISCUSSION

The C-linker/CNBHD of zELK channels forms dimers instead of tetramers as observed in HCN channels¹⁰. A dimeric assembly of the CNBDs was also observed in the crystal structure of the CNBDs of bacterial MlotiK1 channels, however, the C-linker of the MlotiK1 channels consists of only 5 amino acids and is missing the entire “elbow-on-the-shoulder” region characteristic of the eukaryotic channels²⁸. Interestingly, the C-linker/CNBD of HCN2 channels favors dimer over tetramer formation in solution in the absence of cAMP¹⁰, although the multimerization is relatively low affinity. It has been suggested that in the unliganded state HCN channels function as a dimer-of-dimers⁴¹.

What is the quaternary state of the C-linker/CNBHD in intact zELK channels? In principle, the C-linker/CNBHD could form either a dimer-of-dimers (Supplementary Fig. 10a) or a tetramer in intact channels (Supplementary Fig. 10b). In sequence alignments, the amino-terminal end of the C-linker in the structure of zELK is within about six amino acids from the carboxy-termini of the pore-lining inner helices in the structures of KcsA (PDB 1K4C)⁴², MthK (PDB 1LNQ)⁴³, and Kv1.2 (PDB 2A79)⁴⁴ channels. The spacing of the amino termini in the dimer of zELK (~ 19 Å) closely matches the spacing of the carboxy-termini of the adjacent inner helices of Kv1.2 (~ 19 Å) and is intermediate between KcsA (~ 12 Å) and MthK (~ 26 Å) channels. However, in order to accommodate two dimers with appropriate spacing, the dimers would have to be positioned with their amino termini facing each other at a distance of ~ 30 Å between the amino-termini of the adjacent subunits on different dimers (Supplementary Fig. 10a and c). Alternatively, when attached to the S6, the C-linker might assume a conformation closer to the one seen in the structure of HCN channels (Supplementary Fig. 10b and d). This could point to an intrinsic flexibility of the C-linker region that reflects its role in ligand-dependent gating¹⁸. The quaternary state of the C-linker/CNBHD in the intact channel remains to be determined.

- 41 Ulens, C. & Siegelbaum, S.A., Regulation of hyperpolarization-activated HCN channels by cAMP through a gating switch in binding domain symmetry. *Neuron* 40 (5), 959-970 (2003).
- 42 Zhou, Y., Morais-Cabral, J.H., Kaufman, A., & MacKinnon, R., Chemistry of ion coordination and hydration revealed by a K⁺ channel-Fab complex at 2.0 Å resolution. *Nature* 414 (6859), 43-48 (2001).
- 43 Jiang, Y. et al., Crystal structure and mechanism of a calcium-gated potassium channel. *Nature* 417 (6888), 515-522 (2002).
- 44 Long, S.B., Campbell, E.B., & MacKinnon, R., Crystal structure of a mammalian voltage-dependent Shaker family K⁺ channel. *Science* 309 (5736), 897-903 (2005).